
*Institute of Paper Science and Technology*
*Atlanta, Georgia*

**IPST Technical Paper Series Number 857**

# Theory of Dispersed Air Flotation

T.J. Heindel and F. Bloom

May 2000

Submitted to
Encyclopedia of Surface and Colloid Science

## INSTITUTE OF PAPER SCIENCE AND TECHNOLOGY
## PURPOSE AND MISSIONS

The Institute of Paper Science and Technology is an independent graduate school, research organization, and information center for science and technology mainly concerned with manufacture and uses of pulp, paper, paperboard, and other forest products and byproducts. Established in 1929 as the Institute of Paper Chemistry, the Institute provides research and information services to the wood, fiber, and allied industries in a unique partnership between education and business. The Institute is supported by 52 North American companies. The purpose of the Institute is fulfilled through four missions, which are:

- to provide multidisciplinary graduate education to students who advance the science and technology of the industry and who rise into leadership positions within the industry;
- to conduct and foster research that creates knowledge to satisfy the technological needs of the industry;
- to provide the information, expertise, and interactive learning that enables customers to improve job knowledge and business performance;
- to aggressively seek out technological opportunities and facilitate the transfer and implementation of those technologies in collaboration with industry partners.

## ACCREDITATION

The Institute of Paper Science and Technology is accredited by the Commission on Colleges of the Southern Association of Colleges and Schools to award the Master of Science and Doctor of Philosophy degrees.

## NOTICE AND DISCLAIMER

The Institute of Paper Science and Technology (IPST) has provided a high standard of professional service and has put forth its best efforts within the time and funds available for this project. The information and conclusions are advisory and are intended only for internal use by any company who may receive this report. Each company must decide for itself the best approach to solving any problems it may have and how, or whether, this reported information should be considered in its approach.

IPST does not recommend particular products, procedures, materials, or service. These are included only in the interest of completeness within a laboratory context and budgetary constraint. Actual products, materials, and services used may differ and are peculiar to the operations of each company.

In no event shall IPST or its employees and agents have any obligation or liability for damages including, but not limited to, consequential damages arising out of or in connection with any company's use of or inability to use the reported information. IPST provides no warranty or guaranty of results.

# THEORY OF DISPERSED AIR FLOTATION

Theodore J. Heindel

Institute of Paper Science and Technology

500 10th Street, NW

Atlanta, GA 30318-5794

ted.heindel@ipst.edu

Frederick Bloom

Department of Mathematical Sciences

Northern Illinois University

DeKalb, IL 60115

bloom@math.niu.edu

## I INTRODUCTION

Flotation separation is a process used in many industries to separate one constituent from another. Kitchener [1] lists several applications where flotation separation is used. The general process of flotation separation can be divided into two types: (i) dispersed air flotation and (ii) dissolved air flotation [2]. Dispersed air flotation is commonly found in mineral processing (mineral flotation) and paper recycling (flotation deinking). In these processes, relatively large bubbles are formed by mechanical agitation or sparger air injection. Bubble-particle aggregates

then form between bubbles and naturally or chemically-induced hydrophobic particles. Bubbles with sufficient buoyant force carry the particles to the surface for removal. Dispersed air flotation is a selective process in that it separates, for example, hydrophobic mineral or contaminant particles from gangue or desired fiber in mineral flotation and flotation deinking, respectively. In contrast, dissolved air flotation is typically found in water clarification, where air is dissolved into the process stream under pressure. When the pressure is reduced, numerous fine bubbles come out of solution and float "rafts" of aggregated particles to the surface for eventual separation. The aggregated particles are typically colloidal in nature and must be flocculated together before bubble nucleation. Because of this, dissolved air flotation is not considered selective. In this review, the theory of dispersed air flotation will be discussed and dissolved air flotation will not be addressed. Therefore, for the remainder of this review, dispersed air flotation will simply be referred to as "flotation".

Flotation separation is used extensively in mineral processing and many books [3-7] and review articles [1,8-12] are available. Flotation deinking is a separation process used to remove ink and other contaminant particles from reclaimed cellulose fiber. Many reviews of this process are also available [13-18]. A discussion of the similarities and differences between these two flotation separation processes can be found in [18-22].

Despite the many differences between mineral flotation and flotation deinking, all flotation cells operate on similar principles. In modern flotation cells, three separate processes take place in tandem: (i) aeration, where air bubbles are introduced into the system; (ii) mixing, where bubbles and particles are intimately mixed to maximize bubble-particle interaction; and (iii) separation,

where bubbles and bubble-particle aggregates are allowed to separate from the bulk mixture and are skimmed away. The discussion that follows addresses the modeling of this complex process, and is based on the fundamentals of bubble-particle interaction, aggregate formation, and aggregate stability.

## II FLOTATION MODELING

Crozier [6] states that the simplest flotation study involves more than 25 clearly identifiable variables, and over 100 different variables should be considered in a full-scale flotation study. Systematic experimental studies should be completed at high, medium, and low values of each variable to identify the interactions between variables, but this would lead to $3^{100}$ experiments. Because experimental studies like this would be very time consuming and costly, a considerable effort has been made to mathematically model the flotation separation process. However, the complexity of the overall flotation process has prevented the development of a flotation model based on first principles.

Based on experimental observations, the flotation separation process is thought to be analogous to a chemical reactor [8] which can be described by an ordinary differential equation [9]

$$\frac{dn_p^f}{dt} = -k'\left(n_B^f\right)^m\left(n_p^f\right)^n \tag{1}$$

where $n_B^f$ and $n_p^f$ are the concentrations of free bubbles and particles, respectively, t is the flotation time, m and n are the respective orders of reaction, and $k'$ is a pseudo rate constant. Assuming that the reaction is first order [23-26], and that the bubble concentration is constant and that the removed particles represent a small volume [9,10], the rate of change of particle concentration can be assumed to be proportional to the particle concentration

$$\frac{dn_p^f}{dt} = -kn_p^f \tag{2}$$

The rate constant, k, must be determined experimentally and accounts for the lumped effects of the physical, chemical, and surface properties of the system [10]. Many expressions for the rate constant are available in the literature [3,8-10,23-25,27-31], but the specific value is system dependent.

In what has become a common assumption in the attempt to develop a model of the flotation process that is independent of the flotation equipment, the overall macroprocess of flotation separation is thought to be composed of a series of microprocesses. These microprocesses include (i) the approach of a particle to an air bubble and the subsequent interception of that particle by the bubble; (ii) the sliding of the particle along the surface of the thin liquid film that separates the particle from the bubble, which leads to film rupture; (iii) upon film rupture, the formation of a three-phase contact between the bubble, particle, and fluid; and (iv) the stabilization of the bubble-particle aggregate and its transport to the froth layer for removal from

the flotation cell. Each of these microprocesses have probabilities associated with them that they will successfully occur, and these will be discussed in detail in Section III.

Schuhmann [32] assumed that the individual flotation microprocesses were independent. Schulze [3,19,21,33] used this idea and has written Eq. (2) in the form

$$\frac{dn_p^f}{dt} = -ZP_{overall}n_B^f n_p^f \tag{3}$$

where $P_{overall}$ is the overall probability that a stable bubble-particle aggregate will form and be lifted to the froth layer and Z is related to the bubble-particle collision frequency (to be discussed in Section IV). The rate constant in Eq. (3) is

$$k = ZP_{overall}n_B^f \tag{4}$$

The form of Eqs. (1-3) represents a kinetic- or population balance-type model where the population of free particles is modeled. These equations suggest that given a long enough flotation time, all free particles will eventually be removed, which, in practice, may not be realized.

Bloom and Heindel [34-37] have extended the idea of a population balance model to include a forward and reverse reaction (i.e., the birth and death of free particles); this model has the form

$$\frac{dn_p^f}{dt} = -k_1 n_p^f + k_2 n_B^a \tag{5}$$

where $n_B^a$ represents the concentration of bubbles with attached particles. The first term on the right-hand side of Eq. (5) represents the successful formation of a bubble-particle aggregate and its subsequent rise to the froth layer. The second term is a measure of the probability that a bubble-particle aggregate will become unstable before it reaches the froth layer and split to yield a "new" free particle. The kinetic rate constants, $k_1$ and $k_2$, are positive numbers described by

$$k_1 = ZP_{overall} n_B^f \tag{6}$$

and

$$k_2 = Z'P_{destab} = Z'(1 - P_{stab}) \tag{7}$$

where $P_{destab}$ is the probability a bubble-particle aggregate will become unstable, $P_{stab}$ is the probability the bubble-particle aggregate will remain stable, and $Z'$ is the detachment frequency of particles from bubbles.

A model that employs a system of partial differential equations to model free and attached particles in the system has been proposed [3,38]; this system accounts for particle advection and diffusion, as well as particle source and sink terms. Although the coupled general transport

balance equations were presented for free and attached particles, no effort has yet been made to solve them.

## III FLOTATION MICROPROCESSES

In modeling the flotation process, the overall probability that a bubble-particle aggregate will form and be carried to the froth layer ($P_{overall}$) must be determined. Following Schuhmann [32], and assuming the individual microprocess probabilities are independent, it is common to describe $P_{overall}$ by

$$P_{overall} = P_c P_{asl} P_{tpc} P_{stab} \tag{8}$$

where $P_c$ is the probability of bubble-particle collision or capture, $P_{asl}$ is the probability of bubble-particle attachment by sliding, $P_{tpc}$ is the probability of forming a three-phase contact, and $P_{stab}$ is the probability a bubble-particle aggregate will remain stable on its journey to the froth layer. The exact formulation of Eq. (8) may differ from author to author. Some investigators imply $P_{tpc} \approx 1$ and omit this term from $P_{overall}$ [20,25,31,39-43]. Equation (8) assumes that once a bubble-particle aggregate reaches the froth layer, it is removed from the system. A probability may also be associated with the particle removal from the froth layer and an additional term could be added to Eq. (8) [27].

As stated in Section I, mixing is used to maximize bubble-particle interactions, and flotation cells can be assumed to have regions of complex, highly turbulent flows. However, as the distance

separating the particle from the bubble decreases, the flow conditions relative to the bubble-particle pair are typically idealized and simplified to be that of unperturbed flow [41]. This allows for considerable simplifications that are universally applied in modeling the flotation microprocesses.

Models for each microprocess have been developed. Most of these models assume that the bubble and particle are spherical. In addition, most of the microprocess analyses consider the interaction of one particle with one bubble. Efforts to include non-spherical particles [44], multiple particles interacting with a single bubble [45,46], or bubble swarms [45,47], add additional mathematical complications to the modeling process.

## III.A Bubble-Particle Collision

As a particle moves through a flotation cell, it must travel close enough to a bubble for it to be captured. This process is also referred to as collision or interception. When capture occurs, a bubble-particle aggregate does not immediately form, it only implies that short-range forces and thin-film dynamics become significant factors and the second microprocess becomes important. Only those particles which approach a rising bubble within a streaming tube of limiting capture radius, $R_c$, will collide with a bubble (Fig. 1). The probability of collision or capture ($P_c$) is then determined as the ratio of the number of particles with $R_p < R_B$ within a streaming tube of cross-sectional area $\pi R_c^2$ to the number of particles that approach a bubble in a streaming tube with cross-sectional area $\pi(R_p + R_B)^2$

$$P_c = \left( \frac{R_c}{R_B + R_p} \right)^2 \tag{9}$$

Some authors (e.g., [3,33,41]) assume that $R_p \ll R_B$ and write Eq. (9) as

$$P_c = \left( \frac{R_c}{R_B} \right)^2 \tag{10}$$

Two dimensionless parameters are typically encountered when discussing $P_c$, the bubble Reynolds number ($Re_B$) and the Stokes number (St). They are defined as

$$Re_B = \frac{\rho_\ell \upsilon_B d_B}{\mu_\ell} \tag{11}$$

and

$$St = \frac{\rho_p d_p^2 \upsilon_B}{9 \mu_\ell d_B} = \frac{Re_B \rho_p d_p^2}{9 \rho_\ell d_B^2} \tag{12}$$

where $\upsilon_B$ is the bubble rise velocity, $d_B$ and $d_p$ are the bubble and particle diameter, $\rho_p$ and $\rho_\ell$ are the particle and liquid density, and $\mu_\ell$ is the liquid dynamic viscosity. For mineral flotation, $0.1 < St < 1$ is a reasonable assumption, while for flotation deinking, $St < 0.1$ is more typical. For these conditions, inertia forces have a negligible effect on the particle motion and the particles are

assumed to follow the fluid streamlines in the flow field around the bubble (Fig. 1). Hence, the problem of determining $P_c$ is one of identifying the limiting streamline at which the particle will graze the bubble at $\theta = \pi/2$ in Fig. 1. Three flow types are typically addressed when identifying $R_c$: (i) potential flow where $Re_B \rightarrow \infty$; (ii) Stokes flow where $Re_B \rightarrow 0$; and (iii) intermediate flow defined by Yoon and Luttrell [41] where $1 \lesssim Re_B \lesssim 100$. If one does not assume that the grazing trajectory occurs at $\theta = \pi/2$ in Fig. 1, then a collision angle $\theta_c$ must be introduced where $\theta_c$ is the angle on the bubble surface, measured from the front stagnation point, over which particle collision is possible. Cases for which $\theta_c \neq \pi/2$ have been discussed [48-53].

Heindel and Bloom [54] recently considered long-range hydrodynamic forces that act on a particle as it approaches a bubble (i.e., the drag, gravitational, and buoyancy forces), as well as particle settling effects, and developed an exact analytical expression for $P_c$. For the intermediate flow of Yoon and Luttrell [41], Heindel and Bloom [54] determined that

$$P_c^{int} = \frac{1}{1+|G|}\left\{\frac{1}{2\left[\left(\frac{R_p}{R_B}\right)+1\right]^3}\left[2\left(\frac{R_p}{R_B}\right)^3+3\left(\frac{R_p}{R_B}\right)^2\right]\right.$$
$$\left.+\frac{2Re_B^*}{\left[\left(\frac{R_p}{R_B}\right)+1\right]^4}\left[\left(\frac{R_p}{R_B}\right)^3+2\left(\frac{R_p}{R_B}\right)^2\right]\right\}+\frac{|G|}{1+|G|} \qquad (13)$$

where

$$Re_B^* = \frac{1}{15} Re_B^{0.72} \tag{14}$$

and

$$G = \frac{\upsilon_{ps}}{\upsilon_B} \tag{15}$$

with $\upsilon_{ps}$ representing the actual particle settling velocity. The only assumptions used in the development of Eq. (13) were that the bubble and particle are spherical and $R_p < R_B$. The superscript "int" in Eq. (13) implies this is $P_c$ for the intermediate flow of Yoon and Luttrell [41]. For Stokes flow around the bubble, Heindel and Bloom determined that [54]

$$P_c^{st} = \frac{1}{1+|G|}\left\{\frac{1}{2\left[\left(\frac{R_p}{R_B}\right)+1\right]^3}\left[2\left(\frac{R_p}{R_B}\right)^3 + 3\left(\frac{R_p}{R_B}\right)^2\right]\right\} + \frac{|G|}{1+|G|} \tag{16}$$

where "st" denotes Stokes flow conditions. It can also be shown that for potential flow, the exact expression for $P_c$ is

$$P_c^{pot} = \frac{1}{1+|G|}\left\{\frac{1}{\left[\left(\frac{R_p}{R_B}\right)+1\right]^3}\left[\left(\frac{R_p}{R_B}\right)^3 + 3\left(\frac{R_p}{R_B}\right)^2 + 3\left(\frac{R_p}{R_B}\right)\right]\right\} + \frac{|G|}{1+|G|} \tag{17}$$

where "pot" identifies the flow field is potential flow.

If one neglects particle settling effects (i.e., $G \rightarrow 0$) and assumes

$$R_p + R_B \approx R_B \tag{18}$$

and

$$\left(\frac{R_p}{R_B}\right)^3 \ll \left(\frac{R_p}{R_B}\right)^2 \tag{19}$$

then Eq. (13) reduces to

$$P_c^{int} \approx \left(\frac{3}{2} + 4Re_B^*\right)\left(\frac{R_p}{R_B}\right)^2 \tag{20}$$

which is the commonly referenced Yoon and Luttrell expression for $P_c$ [41]. Applying these same assumptions to Eq. (16), $P_c$ for Stokes flow can be approximated as

$$P_c^{st} \approx \frac{3}{2}\left(\frac{R_p}{R_B}\right)^2 \tag{21}$$

which is the often cited value for $P_c$ for Stokes flow conditions. Making a further approximation that

$$\left(\frac{R_p}{R_B}\right)^2 \ll \left(\frac{R_p}{R_B}\right) \tag{22}$$

reduces Eq. (17) to the Sutherland result for potential flow [55]

$$P_c^{pot} \approx 3\left(\frac{R_p}{R_B}\right) \tag{23}$$

Nguyen-Van [48] has developed an accurate correlation for $P_c$ that includes the possibility that $\theta_c < \pi/2$. This correlation has the form

$$P_c^{nv} = \frac{1}{1+|G|}\left(\frac{R_p}{R_B}\right)^2\left[\frac{\sqrt{(X+C)^2+3Y^2}-(X+C)}{13.5Y^2}\right]\left[\sqrt{(X+C)^2+3Y^2}+2(X+C)\right]^2 \tag{24}$$

where

$$C = \frac{2R_B^2(\rho_p - \rho_\ell)g}{9\mu_\ell \upsilon_B} \tag{25}$$

$$X = 1.5\left[1 + \frac{3Re_B/16}{1 + 0.309Re_B^{0.694}}\right] \tag{26}$$

$$Y = \frac{3Re_B/8}{1 + 0.217Re_B^{0.518}} \tag{27}$$

with g the acceleration of gravity. The superscript "nv" in Eq. (24) associates the $P_c$ value with the work in Nguyen-Van [48]. This correlation for $P_c$ is rather complicated, but it follows experimental data very well.

Various $P_c$ predictions are compared in Fig. 2 to data obtained by Nguyen-Van [48] for galena particles. The exact solution for intermediate and Stokes flow bracket the data very well. There is not a significant difference between these two predictions because the particles are very small relative to the bubble. Nguyen-Van's correlation also follows the data extremely well. The exact potential flow solution significantly over predicts $P_c$ and it is well above the $P_c = 0.03$ limit shown in Fig. 2. Since $R_p \ll R_B$ for the conditions in Fig. 2, most of the assumptions used to obtain Eqs. (20), (21), and (23) are satisfied. The one assumption that is not satisfied with this data is a negligible particle settling velocity (due to the large galena density), which implies $G \neq 0$ for this system. Therefore, the Yoon and Luttrell [41] prediction significantly under predicts $P_c$. The approximate expression for Stokes flow severely under predicts the data. The approximate potential flow solution is included in Fig. 2, but it greatly over predicts the data. In summary, the

Nguyen-Van correlation [48] produces the best $P_c$ results, but the correlation is very complicated. The exact analytical solution of Heindel and Bloom [54] for intermediate flow is also a good predictor of $P_c$ and it is easy to use.

## III.B Bubble-Particle Attachment by Sliding

Not all particles that are captured by a bubble become attached. In general, only particles that are sufficiently hydrophobic (either naturally or chemically-induced) are able to attach themselves to a bubble through a formation of a three-phase contact [41]. Before the three-phase contact occurs, the liquid layer between the bubble and particle, which forms as soon as the particle is captured by the bubble, must thin sufficiently to rupture. This liquid layer is typically referred to as a liquid (disjoining) film and thin-film dynamics have been used to describe the rupture process [3,9,25,26,40,56-63].

Upon liquid film formation, the particle begins to slide over the bubble surface and resides on it for a finite time period, referred to as the sliding time, $\tau_{sl}$. This sliding process subjects the disjoining film to a weak surface deformation, which tends to thin the film out and may lead to film rupture. For bubble-particle attachment to occur during sliding, defined as attachment by sliding, the contact time of the particle with the liquid film must be greater than the induction (or drainage) time, $\tau_i$, of the film up to the point of film rupture. This microprocess has been identified by some as the most important microprocess in flotation [9,20,56], and it is probably the most complex and least understood.

The probability of attachment by sliding, $P_{asl}$, is determined from knowledge of the location where the particle touches the bubble and the sliding process. If $h_0$ is defined as the initial disjoining film thickness (Fig. 3) and $h_{crit}$ is the critical film thickness that the film must reach in order for rupture to occur, then the critical position angle $\phi^*_{crit}$ is defined as the largest touching angle $\phi_T$ (< 90°) such that $h = h_{crit}$ will be achieved at a position angle $\phi_{crit}$ with $\phi_T < \phi_{crit} \leq \pi/2$. If the touching angle is less than the critical position angle, the sliding time will be sufficient for film rupture. Therefore, all particles that satisfy $\phi_T \leq \phi^*_{crit}$ will attach to the bubble, and those particles that touch the bubble with $\phi_T > \phi^*_{crit}$ will not. Referring to Fig. 3, $P_{asl}$ is typically described to be the ratio of the area inscribed by the limiting radius $R_{crit}$ (the radius from the stagnation line to the line corresponding to the touching angle associated with $\phi^*_{crit}$), to the area inscribed by $R_B + R_p + h_{crit}$. Since it is assumed that $h_{crit} \ll R_p$, $P_{asl}$ can be written as [33,41,64]

$$P_{asl} = \frac{R_{crit}^2}{(R_B + R_p)^2} \tag{28}$$

Relating $R_{crit}$ to $\phi^*_{crit}$, Eq. (28) assumes the form

$$P_{asl} = \sin^2 \phi^*_{crit} \tag{29}$$

Equation (29) assumes that the largest possible touching angle occurs precisely at $\phi_{T,max} = \pi/2$ (i.e., the liquid flow around the bubble has fore and aft symmetry). If the flow is not symmetric, $\phi_{T,max} < \pi/2$ and Eq. (29) must be modified to [26,53,57,61]

$$P_{asl} = \frac{\sin^2 \phi^*_{crit}}{\sin^2 \phi_{T,max}} \tag{30}$$

To determine $\phi^*_{crit}$, a coupled set of differential equations must be formulated and solved that relate $\phi$, the particle position angle relative to the stagnation point, with h, the disjoining film thickness [65]. In developing this system of equations, it is commonly assumed that [33,64]: (i) the particle moves in a quasi-stationary manner in an almost circular path along the bubble surface; (ii) the sliding length $L \gg h$ and $dL/dt > dh/dt$; (iii) for $0 < \phi < \pi/2$, the influence of the fluid boundary layer around the bubble is negligible; and (iv) the velocity field around the bubble is given by potential flow for the case of an unretarded bubble surface and by the intermediate flow of Yoon and Luttrell [41] for the case of a completely retarded bubble surface. In flotation systems, surface active agents are commonly found in the fluid medium; these coat and immobilize the bubble surface which causes the bubbles to act like rigid spheres. However, recent work [43,57] has suggested that the surface active agents are swept to the lower hemisphere of the bubble surface as it rises through the fluid, causing the upper hemisphere to be free of surface active agents and completely mobile.

To describe the particle motion as it slides over the bubble surface, Schulze [33,64] has completed a force balance about the particle. For quasi-static conditions, the radial force balance yields

$$-F_{gr} + F_c + F_L - F_{ur} + F_T = 0 \tag{31}$$

where $F_{gr}$ is the radial component of the particle weight, $F_c$ is the centrifugal force exerted on the particle, $F_L$ is the lift force on the particle, $F_{ur}$ is the radial component of the flow force acting on the particle in the vicinity of the bubble, and $F_T$ is the resistive force generated during the drainage of the disjoining film.

The magnitude of the radial component of the particle weight is determined from

$$F_{gr} = \frac{4}{3}\pi R_p^3 \Delta\rho g \cos\phi \tag{32}$$

where $\Delta\rho = \rho_p - \rho_\ell$ and $\phi$ is the particle position angle measured from the stagnation streamline. The centrifugal force acting on the particle has the form

$$F_c = \frac{4}{3r}\pi R_p^3 \Delta\rho \left(\upsilon_{p\phi}^{rel}\right)^2 \tag{33}$$

where $r = R_p + R_B + h$ and $\upsilon_{p\phi}^{rel}$ is the tangential particle velocity relative to the bubble (see Bloom and Heindel [65] for a discussion concerning $\upsilon_{p\phi}^{rel}$). The centrifugal force has been shown to be small relative to the other radial forces and it may be neglected in the radial force balance [42,65].

Schulze [33,64] has used the result presented by Saffman [66] to describe the lift force experienced by a particle as it slides over the disjoining film. This force is determined from

$$F_L = 3.24\mu_\ell R_p \upsilon_{p\phi}^{rel} \sqrt{Re_S} \tag{34}$$

where the shear Reynolds number is defined by

$$Re_S = \frac{4R_p^2}{\nu_\ell}\frac{\partial u_\phi}{\partial r} \tag{35}$$

with $\nu_\ell$ the liquid kinematic viscosity and $u_\phi$ the tangential component of the fluid velocity. Bloom and Heindel [65] have shown this expression for $F_L$ is valid for selected conditions associated with mineral flotation, but invalid for conditions affiliated with flotation deinking. Several investigators [42,65,67,68] have reasoned that $F_L$ plays only a minor role in the particle force balance and have neglected it all together in their derivation of $P_{asl}$.

The radial component of the flow force acting on the particle is given by [67]

$$F_{ur} = 6\pi\mu_\ell R_p |u_r| \tag{36}$$

For the intermediate flow of Yoon and Luttrell [41],

$$u_r = \upsilon_B k(r)\cos\phi \tag{37}$$

where

$$k(r) = -\left[\left(1 - \frac{3R_B}{2r} + \frac{R_B^3}{2r^3}\right) + 2Re_B^*\left(\frac{R_B^4}{r^4} - \frac{R_B^3}{r^3} - \frac{R_B^2}{r^2} + \frac{R_B}{r}\right)\right] \tag{38}$$

with $r = R_B + R_p + h$. Equation (36) has been modified by Bloom and Heindel [65] to account for particle settling effects; this expression is given by

$$F_{ur} = \frac{6\pi\mu_\ell R_p \upsilon_B}{\lambda}|k(r)|\cos\phi \tag{39}$$

where $\lambda$ is given in terms of the particle Reynolds number ($Re_p$) and the Archimedes number (Ar):

$$\lambda = 18\frac{Re_p}{Ar} \tag{40}$$

with

$$Ar = \frac{\Delta\rho d_p^3 g}{\rho_\ell \nu_\ell^2} \tag{41}$$

The final force in Eq. (31) is the resistive force generated during film drainage, $F_T$. This force is often attributed to the disjoining pressure between the bubble and particle [3,24,40,56,58,60] and can be determined from

$$F_T = \int_{S_B} P dS_B \tag{42}$$

where P is the disjoining film pressure and $S_B$ is the bubble surface area. By including only the capillary pressure in the disjoining film pressure, $F_T$ has been shown to be [3,34,58]

$$F_T = \frac{6\pi\mu_\ell R_p^2 \upsilon_{pr}}{hC_B} \tag{43}$$

where $\upsilon_{pr}$ is the radial component of the particle velocity and $C_B$ characterizes the degree of bubble surface immobilization due to the presence of surface active agents. The parameter $C_B$ varies between one (for a completely immobilized or rigid bubble surface) and four (for a completely unrestrained bubble surface).

Equation (43), along with Eqs. (32) and (39), were recently used by Bloom and Heindel [65] to obtain a closed-form approximation for $P_{asl}$. The approximation has the form

$$P_{asl} = \exp\left\{-2\left(\frac{\lambda}{C_B}\right)\left(\frac{R_p}{R_B + R_p}\right)\left[\frac{g(r) - G}{|k(r)| - G}\right]\left(\frac{h_0}{h_{crit}} - 1\right)\right\} \tag{44}$$

where $\lambda$ is given by Eq. (40), G is given by Eq. (15), and for the intermediate flow of Yoon and Luttrell [41], k(r) is given by Eq. (38) with $r \approx R_B + R_p$, while g(r) is given by

$$g(r) = \left(1 - \frac{3R_B}{4r} - \frac{R_B^3}{4r^3}\right) + Re_B^* \left(\frac{R_B}{r} + \frac{R_B^3}{r^3} - \frac{2R_B^4}{r^4}\right) \tag{45}$$

The expression for $P_{asl}$ in Eq. (44) accounts for surface tension effects in the disjoining film and includes particle settling effects. However, this form does not account for additional forces that contribute to the disjoining film pressure. The actual form of the disjoining film pressure is still under debate [3,25,40,56], but it has recently been suggested that the disjoining pressure can be described by [56]

$$P = -\sigma \frac{\partial^2 h}{\partial x^2} - \frac{A}{h^3} \pm B \frac{e^{-\kappa h}}{1 - e^{-\kappa h}} + K_s e^{-h/d} \tag{46}$$

The first term in Eq. (46) accounts for the surface tension effects with $\sigma$ the surface tension; the second term addresses London-van der Waals dispersion effects with A proportional to the Hamaker constant; the third term is influenced by electrostatic interactions, where B is related to the strength of the electrostatic interaction and $1/\kappa$ is the double layer thickness; the fourth term describes the hydrophobic attraction effects, where $K_s$ is related to this attraction and d is the decay length which is proportional to the hydrophobic attraction length scale. The complexity of Eq. (46) has prevented obtaining a closed form expression for $F_T$ by using Eq. (42); however, if all the constants are known, numerical solutions are possible.

The critical attachment angle, $\phi_{crit}^*$, has also been defined as that angle at which the particle touches the bubble where the particle sliding time over the bubble surface is exactly equal to the

induction time. Therefore, $\phi^*_{crit}$ relates both the sliding time and induction times to $P_{asl}$ [57]. Several expressions for sliding time and/or induction time are available in the literature [26,41,53,57,61,68,69]. Yoon and Luttrell [41] present $P_{asl}$ expressions in terms of particle induction time for Stokes, intermediate, and potential flow conditions. For example, for intermediate flow, they present [41]

$$P_{asl} = \sin^2\left\{2\arctan\left[\exp\left(\frac{-(45+8Re_B^{0.72})\upsilon_B\tau_i}{30R_B(R_B/R_p+1)}\right)\right]\right\} \tag{47}$$

where $\tau_i$ is the induction time. Nguyen et al. [26] have recently measured induction times for various experimental conditions and showed that $\tau_i$ typically ranged from 2 to 10 milliseconds.

## III.C Bubble-Particle Three-Phase Contact

Once the thin film separating the bubble from the particle has ruptured, a sufficiently large three-phase contact (TPC) between the liquid, particle, and bubble must form; this must happen within a relatively short time period ($\tau_{tpc}$) in order to provide a strong enough attachment force that will prevent the bubble-particle aggregate from immediately separating. If $\tau_v$ represents the average lifetime of turbulent vortices within a flotation cell, then the time required for a three-phase contact to form and create a bubble-particle aggregate must satisfy $\tau_{tpc} < \tau_v$. Schulze [33] has used the ratio $\tau_v/\tau_{tpc}$ to define the probability of the formation of a three-phase contact

$$P_{tpc} \approx 1 - \exp\left(\frac{-\tau_v}{\tau_{tpc}}\right) \tag{48}$$

It has been suggested that if the film separating the bubble from the particle does rupture, the formation of a bubble-particle aggregate (i.e., a three-phase contact) is almost certain [8]. Schulze [33] tabulated values of $P_{tpc}$ for 10 μm ≤ $R_p$ ≤ 100 μm and showed that $P_{tpc} \approx 1$, which supports the claim of almost certain bubble-particle aggregate formation. Indeed, many authors assume $P_{tpc} = 1$ and omit this term from $P_{overall}$ [20,25,31,39-43].

It has also been suggested that formation of a three-phase contact is part of the attachment by sliding process [26,40,61,70]. This is implied by including $\tau_{tpc}$ as a small portion of the total induction time, $\tau_i = \tau_F + \tau_{tpc}$, where $\tau_F$ is defined as the film drainage time [40,70,71]. As noted by Nguyen et al. [26], the effect of liquid rupture and formation of a three-phase contact has received the least attention relative to the other flotation microprocesses and it requires deeper experimental and theoretical investigation.

## III.D Bubble-Particle Aggregate Stability

After a bubble-particle aggregate forms, it must remain stable on its journey to the froth layer in order to be removed from the system. It is generally accepted [3,9,24,33,46,72-74] that bubble-particle aggregate stability can be estimated by performing a quasi-static force balance on the bubble-particle aggregate. These forces are schematically represented in Fig. 4. The net detachment force that acts on the bubble-particle aggregate is given by

$$F_{detach} = F_{wt} + F_d + F_\sigma \tag{49}$$

where $F_{wt}$ is the apparent weight of the bubble-particle aggregate and composed of the bubble buoyancy force ($F_b$) and the particle gravitational force ($F_g$), $F_d$ is the fluid drag force, and $F_\sigma$ is the capillary pressure force. The net attachment force on the bubble-particle aggregate is

$$F_{attach} = F_{ca} + F_{hyd} \tag{50}$$

where $F_{ca}$ is the capillary force and $F_{hyd}$ is the hydrostatic force. The derivation of these forces are available in the literature [3,24,33,72-74].

To determine the apparent bubble-particle aggregate weight, the bubble buoyant force and particle gravitation force are combined to yield

$$F_{wt} = F_g - F_b = \frac{4}{3}\pi R_p^3(\rho_p - \rho_\ell)g \tag{51}$$

The fluid drag force is approximated by

$$F_d \approx \frac{4}{3}\pi R_p^3 \rho_p a_c \tag{52}$$

where $a_c$ is the particle acceleration which depends on the overall flotation cell flow conditions. Schulze [33] has estimated that

$$a_c \approx \frac{1.9\varepsilon^{2/3}}{(R_B + R_p)^{1/3}} \tag{53}$$

when aggregates are moved by the centrifugal acceleration generated in the flow external to vortices in the inertial region, where $\varepsilon$ is the turbulent energy density. The capillary pressure force is estimated from

$$F_\sigma = \pi R_p^2 \left( \frac{2\sigma}{R_B} - 2R_B \rho_\ell g \right) \sin^2 \omega \tag{54}$$

where $\sigma$ is the surface tension and $\omega$ is the angle identified in Fig. 4. The capillary force that contributes to particle detachment is given by

$$F_{ca} = -2\pi R_p \sigma \sin\omega \sin(\omega + \theta) \tag{55}$$

where $\theta$ is the (static) contact angle. The hydrostatic pressure force from the liquid height $z_0$ above the contact radius $r_p = R_p \sin\omega$ is

$$F_{hyd} = \pi R_p^2 \rho_\ell g z_0 \sin^2 \omega \tag{56}$$

Using the experimental results of Plate [75], Schulze [33] reasoned that the probability of stability should be of the form

$$P_{stab} = 1 - \exp\left(1 - \frac{F_{attach}}{F_{detach}}\right) \tag{57}$$

Bloom and Heindel [36] recently used this form of $P_{stab}$ in comparisons between predicted and experimental bench-top flotation deinking results. They determined that an empirical constant must be included in Eq. (57) to match the experimental data; their form for $P_{stab}$ is

$$P_{stab} = 1 - \exp\left[A_s\left(1 - \frac{F_{attach}}{F_{detach}}\right)\right] \tag{58}$$

where $A_s$ is an empirical constant that varies between 0 and 1 and is thought to be system dependent. The constant $A_s$ in Eq. (58) has the value of $A_s = 1$ in Schulze [33]. Further research into the proper form of $P_{stab}$ is required.

## IV COLLISION AND DETACHMENT RATES

Collision "frequencies" are associated with the kinetic constants in the flotation models described by Eq. (3) or (5). The parameter identified as Z (Eq. (4) and (6)) is not a true frequency because it has units of volume per unit time. However, the quantity $Zn_B^f$ produces a true collision frequency and controls the rate of bubble-particle aggregate formation. The detachment

frequency $Z'$ (Eq. (7)) controls the rate of bubble-particle aggregate break-up in the flotation cell. Bloom and Heindel [76] recently reviewed various models associated with the bubble-particle aggregate collision and detachment processes.

Many different expressions for the collision rate between two particles ($Z_{12}$) moving through a fluid stream have appeared in the literature. Most are based on the work of von Smoluchowski [77] for the colloidal particle collision process; it was proposed that

$$Z_{12} = \frac{4}{3} N_1 N_2 d_{12}^3 V_g \tag{59}$$

where $N_i$ is the particle concentration of species i, $d_{12}$ is the sum of the particle radii associated with the two species, and $V_g$ is the velocity gradient perpendicular to the direction of particle motion. This expression for $Z_{12}$ assumes a randomly distributed suspension of colloidal particles in a fluid moving under uniform shear, with the particles following the fluid streamlines up to the moment of impact as if no other particles were present. Camp and Stein [78] extended this work to turbulent flows to obtain

$$Z_{12} = \frac{4}{3} N_1 N_2 d_{12}^3 \left( \frac{\varepsilon}{\nu_\ell} \right)^{1/2} \tag{60}$$

Saffman and Turner [79] obtained similar results.

Abrahamson [80] developed an expression for $Z_{12}$ that allows for a Gaussian distribution of particle velocities. This expression can be used to determine Z, the bubble-particle collision "frequency" in flotation cells, and has the form [76,80]

$$\begin{aligned} Z &= Z_{12} / N_1 N_2 \\ &\cong 5.0(R_B + R_p)^2 \sqrt{U_p^2 + U_B^2} \end{aligned} \tag{61}$$

where $U_p$ and $U_B$ are the effective values of the relative velocities between the particle and fluid and bubble and fluid, respectively; these values are given by [81]

$$U_p = 0.4 \frac{\varepsilon^{4/9} d_p^{7/9}}{\nu_\ell^{1/3}} \left( \frac{\rho_p - \rho_\ell}{\rho_\ell} \right)^{2/3} \tag{62}$$

and

$$U_B = 0.4 \frac{\varepsilon^{4/9} d_B^{7/9}}{\nu_\ell^{1/3}} \left( \frac{|\rho_B - \rho_\ell|}{\rho_\ell} \right)^{2/3} \tag{63}$$

Equation (61) does not account for particle settling effects; when these effects are included in the formulation, it can be shown that [76,80]

$$Z = 5.0(R_B + R_p)^2 \sqrt{U_p^2 + U_B^2}\, \exp\left[ -\frac{1}{2} \frac{\left(|\upsilon_{ps}| + \upsilon_B\right)^2}{U_p^2 + U_B^2} \right] + \pi(R_B + R_p)^2 \left\{ \frac{\left(|\upsilon_{ps}| + \upsilon_B\right)^2 + U_p^2 + U_B^2}{|\upsilon_{ps}| + \upsilon_B} \operatorname{erf}\left[ \frac{|\upsilon_{ps}| + \upsilon_B}{\sqrt{2\left(U_p^2 + U_B^2\right)}} \right] \right\} \tag{64}$$

where erf(x) is the standard error function. Bloom and Heindel [76] have compared predictions for Z with and without particle settling effects; they showed that particle settling effects increase the predicted Z value by approximately 1.5 times.

The concept of bubble-particle detachment has been likened to floc disruption [76]. Following Mika and Fuerstenau [82], Bloom and Heindel [76] proposed that $Z'$ can be estimated from

$$Z' = \frac{\sqrt{C_1}\varepsilon^{1/3}}{(d_p + d_B)^{2/3}} \tag{65}$$

where $C_1$ is an empirical constant with a range $1.61 \leq C_1 \leq 2.33$.

## V SUMMARY

Dispersed air flotation is a selective separation process that is used in many industries. Models of the overall flotation process have been presented. These models are based on the assumption that the process can be likened to a first-order kinetic reaction or population balance model. The kinetic constants in these models have been formulated from knowledge of the fundamentals of

bubble-particle interaction, aggregate formation, and aggregate stability. The overall probability that a bubble-particle aggregate will form and be removed to the flotation cell froth layer is composed of a series of independent microprocess probabilities. In sequential order, these include (i) the probability of particle capture or collision ($P_c$); (ii) the probability of particle attachment by sliding ($P_{asl}$); (iii) the probability of three-phase contact ($P_{tpc}$); and (iv) the probability of bubble-particle aggregate stability ($P_{stab}$). The details of each microprocess have been discussed. Collision and detachment rate models have also been summarized. With a knowledge of these fundamentals, it is hoped that improvements in flotation separation efficiencies can be realized.

## VI ACKNOWLEDGMENT

Portions of this work were funded by the member companies of the Institute of Paper Science and Technology, Atlanta, GA. Their support is gratefully acknowledged.

## VII NOMENCLATURE LIST

| | | |
|---|---|---|
| A | - | constant proportional to the Hamaker constant |
| $A_s$ | - | constant in Eq. (58) |
| Ar | - | Archimedes number |
| $a_c$ | - | particle acceleration |
| B | - | constant related to the strength of the electrostatic interaction |
| C | - | Eq. (25) |

$C_1$ - constant in Eq. (65)

$C_B$ - bubble surface mobility coefficient

d - decay length which is proportional to the hydrophobic attraction length scale

$d_{12}$ - sum of two particle radii

$d_B$ - bubble diameter

$d_p$ - particle diameter

$F_{attach}$ - net attachment force on a bubble-particle aggregate

$F_b$ - bubble buoyant force

$F_c$ - centrifugal force

$F_{ca}$ - capillary force

$F_d$ - fluid drag force

$F_{detach}$ - net detachment force on a bubble-particle aggregate

$F_g$ - particle weight

$F_{gr}$ - radial component of the particle weight

$F_{hyd}$ - hydrostatic force

$F_L$ - particle lift

$F_T$ - resistive force during film drainage

$F_{ur}$ - radial component of the flow force

$F_{wt}$ - apparent bubble-particle aggregate weight

$F_\sigma$ - capillary pressure force

G - Eq. (15)

g - acceleration due to gravity

g(r) - Eq. (45)

$h$ - film thickness

$h_0$ - initial film thickness

$h_{crit}$ - critical film thickness

$K_s$ - constant related to the hydrophobic attraction force

$k$ - flotation rate constant

$k'$ - pseudo rate constant

$k_1$ - flotation rate constant associated with the successful formation of a bubble-particle aggregate and its removal to the froth layer

$k_2$ - flotation rate constant associated with the destabilization of a bubble-particle aggregate

$k(r)$ - Eq. (38)

$L$ - particle sliding length

$m$ - order of reaction

$N_1, N_2$ - particle concentration of species i

$n$ - order of reaction

$n_B^a$ - concentration of bubbles with attached particles

$n_B^f$ - concentration of bubbles without particles

$n_p^f$ - concentration of free particles (i.e., particles not attached to bubbles)

$P$ - disjoining pressure

$P_{asl}$ - probability of bubble-particle attachment by sliding

$P_c$ - probability of bubble-particle collision

$P_{destab}$ - probability of bubble-particle aggregate destabilization

$P_{overall}$ - overall probability a stable bubble-particle aggregate will form and be lifted to the froth layer

$P_{stab}$ - probability of bubble-particle stability

$P_{tpc}$ - probability of forming a three-phase contact

$R_B$ - bubble radius

$R_c$ - limiting capture radius

$R_{crit}$ - radius defined in Fig. 3

$R_p$ - particle radius

$Re_B$ - bubble Reynolds number

$Re_B^*$ - Eq. (14)

$Re_p$ - particle Reynolds number

$Re_S$ - shear Reynolds number

$r$ - $R_p + R_B + h \approx R_p + R_B$

$r_p$ - contact radius defined in Fig. 4

$S_B$ - bubble surface area

St - Stokes number

$t$ - time

$U_B$ - relative velocity between a bubble and the surrounding fluid

$U_p$ - relative velocity between a particle and the surrounding fluid

$u_r$ - radial component of the fluid velocity

$u_\phi$ - tangential component of the fluid velocity

$V_g$ - velocity gradient perpendicular to the direction of particle motion

$X$ - Eq. (26)

$Y$ - Eq. (27)

$Z$ - bubble-particle collision "frequency"

$Z'$ - bubble-particle detachment frequency

$Z_{12}$ - collision rate between two particles

$z_0$ - height defined in Fig. 4

$\varepsilon$ - turbulent energy density

$\theta$ - angle defined in Fig. 1; static contact angle

$\theta_c$ - collision angle

$\kappa$ - inverse of the double layer thickness

$\lambda$ - Eq. (40)

$\mu_\ell$ - liquid dynamic viscosity

$\nu_\ell$ - liquid kinematic viscosity

$\rho_B$ - bubble density

$\rho_\ell$ - liquid density

$\rho_p$ - particle density

$\Delta\rho$ - $\rho_p - \rho_\ell$

$\sigma$ - surface tension

$\tau_F$ - film drainage time

$\tau_i$ - induction time

$\tau_{sl}$ - particle sliding time

$\tau_{tpc}$ - time to form a three-phase contact

$\tau_v$ - average lifetime of a turbulent vortice

$\upsilon_B$ - bubble rise velocity

$\upsilon_{pr}$ - radial component of the particle velocity

$\upsilon_{ps}$ - particle settling velocity

$\upsilon_{p\phi}^{rel}$ - tangential particle velocity relative to the bubble

$\phi$ - particle position angle during sliding

$\phi_{crit}$ - position angle when $h_{crit}$ is reached

$\phi_{crit}^{*}$ - largest touching angle for attachment by sliding to occur

$\phi_T$ - touching angle where sliding begins

$\phi_{T,max}$ - maximum touching angle

$\omega$ - angle defined in Fig. 4

## VIII REFERENCES

1. Kitchener, J.A. The Froth Flotation Process: Past, Present, and Future in Brief. In *The Scientific Basis of Flotation*, Ives, K.J., Ed.; Martinus Nijhoff Publishers: The Hague, 1984; 3-51.

2. Collins, G.L.; Jameson, G.J. Experiments on the Flotation of Fine Particles: The Influence of Particle Size and Charge. Chem. Eng. Sci. **1976**, *31*, 985-991.

3. Schulze, H.J. *Physico-chemical Elementary Processes in Flotation*, Elsevier: Berlin, 1984.

4. Ives, K.J., Ed. *The Scientific Basis of Flotation*, Martinus Nijhoff Publishers: The Hague, 1984.

5. Finch, J.A.; Dobby, G.S. *Column Flotation*, Pergamon Press: Oxford, 1990.

6. Crozier, R.D. *Flotation Theory, Reagents, and Ore Testing*, Pergamon Press: New York, 1992.

7. Matis, K.A., Ed. *Flotation Science and Engineering*, Marcel Dekker, Inc.: New York, 1995.

8. Jameson, G.J.; Nam, S.; Moo Young, M. Physical Factors Affecting Recovery Rates in Flotation. Miner. Sci. Eng. **1977**, *9* (3), 103-118.

9. Ahmed, N.; Jameson, G.J. Flotation Kinetics. Miner. Process. Extract. Metal. Rev. **1989**, *5*, 77-99.

10. Gochin, R.J. Flotation. In *Solid-Liquid Separation*, Svarovsky, L., Ed.; Butterworths: London, 1990; 591-613.

11. Finch, J.A.; Dobby, G.S. Column Flotation: A Selected Review Part I. Int. J. Miner. Process. **1991**, *33*, 343-354.

12. Finch, J.A.; Uribe-Salas, A.; Xu, M. Column Flotation. In *Flotation Science and Engineering*, Matis, K.A., Ed.; Marcel Dekker, Inc.: New York, 1995; 291-330.

13. Ortner, H.E. *Recycling of Papermaking Fibers: Flotation Deinking*, TAPPI Press: Atlanta, GA, 1981.

14. Ferguson, L.D. Deinking Chemistry. In *1995 Deinking Short Course*, Vancouver, WA, June 4-7, 1995; TAPPI Press: Atlanta, GA, 1995; Chapter 6.

15. Ferguson, L.D. Flotation Deinking Technology. In *1995 Deinking Short Course*, Vancouver, WA, June 4-7, 1995; TAPPI Press: Atlanta, GA, 1995; Chapter 10.

16. Eriksson, T.P.; McCool, M.A. A Review of Flotation Deinking Cell Technology. In *Paper Recycling Challenge: Vol. II - Deinking and Bleaching*, Doshi, M.R., Dyer, J.M., Eds.; Doshi & Associates, Inc.: Appleton, WI, 1997; 69-84.

17. Somasundaran, P.; Zhang, L.; Krishnakumar, S.; Slepetys, R. Flotation Deinking - A Review of the Principles and Techniques. Prog. Pap. Recycl. **1999**, *8* (3), 22-36.

18. Heindel, T.J. Fundamentals of Flotation Deinking. TAPPI J. **1999**, *82* (3), 115-124.

19. Schulze, H.J. The Fundamentals of Flotation Deinking in Comparison to Mineral Flotation. In *1st Research Forum on Recycling*, Toronto, October 29-31, 1991; CPPA Press: Toronto, 1991; 161-167.

20. Schulze, H.J. Comparison of the Elementary Steps of Particle/Bubble Interaction in Mineral and Deinking Flotation. In *8th International Conference on Colloid and Surface Science*; 1994.

21. Schulze, H.J. Zur Hydrodynamik der Flotations-Elementarvorgänge. Wochenbl. Papierfabr. **1994**, *122* (5), 160, 162, 164-168.

22. Pan, R.; Paulsen, F.G.; Johnson, D.A.; Bousfield, D.W.; Thompson, E.V. A Global Model for Predicting Flotation Efficiencies: Model Results and Experimental Studies. In *1993 Pulping Conference Proceedings*, TAPPI Press: Atlanta, GA, 1993; 1155-1164.

23. Woodburn, E.T. Mathematical Modelling of Flotation Processes. Miner. Sci. Eng. **1970**, *2*, 3-17.

24. Ralston, J. The Influence of Particle Size and Contact Angle in Flotation. In *Colloid Chemistry in Mineral Processing*, Laskowski, J.S., Ralson, J., Eds.; Elsevier: Amsterdam, 1992; 203-233.

25. Yoon, R.-H.; Mao, L. Application of Extended DLVO Theory, IV - Derivation of Flotation Rate Equation from First Principles. J. Colloid Interface Sci. **1996**, *181*, 613-626.

26. Nguyen, A.V.; Ralston, J.; Schulze, H.J. On Modelling of Bubble-Particle Attachment Probability in Flotation. Int. J. Miner. Process. **1998**, *53*, 225-249.

27. Dorris, G.M.; Pagé, M. Deinking of Toner-Printed Papers. Part I: Flotation Kinetics, Froth Stability and Fibre Entrainment. J. Pulp Pap. Sci. **1997**, *23* (5), J206-J215.

28. Julien Saint Amand, F. Hydrodynamics of Flotation: Experimental Studies and Theoretical Analysis. In *1997 TAPPI Recycling Symposium*, TAPPI Press: Atlanta, GA, 1997; 219-241.

29. Luttrell, G.H.; Yoon, R.H. A Flotation Column Simulator Based on Hydrodynamic Principles. Int. J. Miner. Process. **1991**, *33*, 355-368.

30. Schmidt, D.C.; Berg, J.C. The Selective Removal of Toner Particles from Repulped Slurries by Flotation. In *3rd Research Forum on Recycling*, Vancouver, BC, November 20-22, 1995; CPPA Press: Toronto, 1995; 227-230.

31. Schmidt, D.C.; Berg, J.C. The Effect of Particle Shape on the Flotation of Toner Particles. Prog. Pap. Recycl. **1996**, *5* (2), 67-77.

32. Schuhmann, R. Flotation Kinetics I. J. Phys. Chem. **1942**, *46*, 891-902.

33. Schulze, H.J. Flotation as a Heterocoagulation Process: Possibilities of Calculating the Probability of Flotation. In *Coagulation and Flocculation*, Dobias, B., Ed.; Marcel Dekker, Inc.: New York, 1993; 321-353.

34. Bloom, F.; Heindel, T.J. Mathematical Modelling of the Flotation Deinking Process. Math. Comp. Model. **1997**, *25* (5), 13-58.

35. Bloom, F.; Heindel, T.J. A Theoretical Model of Flotation Deinking Efficiency. J. Colloid Interface Sci. **1997**, *190*, 182-197.

36. Bloom, F.; Heindel, T.J. Lower Bounds for Efficiency in a Semi-Batch Flotation Deinking Model. In Preparation.

37. Heindel, T.J.; Bloom, F. New Measures for Maximizing Ink Particle Removal in a Flotation Cell. In *1997 TAPPI Recycling Symposium*, TAPPI Press: Atlanta, GA, 1997; 101-113.

38. Plate, H.; Schulze, H.J.. Modeling of the Overall Flotation Process Based on Physico-Chemical Microprocesses - Technique and Application. In *XVII International Mineral Processing Congress*, Dresden, September 23-28, 1991; 365-377.

39. Pan, R.; Paulson, F.G.; Johnson, D.A.; Bousfield, D.W.; Thompson, E.V. A Global Model for Predicting Flotation Efficiency Part I: Model Results and Experimental Studies. TAPPI J. **1996**, *79* (4), 177-185.

40. Paulsen, F.G.; Pan, R.; Bousfield, D.W.; Thompson, E.V. The Dynamics of Bubble/Particle Attachment and the Application of Two Disjoining Film Rupture Models to Flotation: I. Nondraining Model. J. Colloid Interface Sci. **1996**, *178*, 400-410.

41. Yoon, R.H.; Luttrell, G.H. The Effect of Bubble Size on Fine Particle Flotation. Miner. Process. Extract. Metal. Rev. **1989**, *5*, 101-122.

42. Mileva, E. Solid Particle in the Boundary Layer of a Rising Bubble. Colloid Polym. Sci. **1990**, *268*, 375-383.

43. Dai, Z.; Dukhin, S.; Fornasiero, D.; Ralston, J. The Inertial Hydrodynamic Interaction of Particles and Rising Bubbles with Mobile Surfaces. J. Colloid Interface Sci. **1998**, *197*, 275-292.

44. Schmidt, D.C.; Berg, J.C. A Preliminary Hydrodynamic Analysis of the Flotation of Disk-Shaped Toner Particles. Prog. Pap. Recycl. **1997**, *6* (2), 38-49.

45. Yianatos, J.B.; Finch, J.A.; Dobby, G.S.; Xu, M. Bubble Size Estimation in a Bubble Swarm. J. Colloid Interface Sci. **1988**, *126* (1), 37-44.

46. Vinke, H.; Hamersma, P.J.; Fortuin, J.M.H. Particle-to-Bubble Adhesion in Gas/Liquid/Solid Slurries. AIChE J. **1991**, *37* (12), 1801-1809.

47. Flint, L.R.; Howarth, W.J. The Collision Efficiency of Small Particles with Spherical Air Bubbles. Chem. Eng. Sci. **1971**, *26*, 1155-1168.

48. Nguyen-Van, A. The Collision Between Fine Particles and Single Air Bubbles in Flotation. J. Colloid Interface Sci. **1994**, *162*, 123-128.

49. Nguyen-Van, A.; Kmet, S. Collision Efficiency for Fine Mineral Particles with Single Bubble in a Countercurrent Flow Regime. Int. J. Miner. Process. **1992**, *35* (3/4), 205-223.

50. Weber, M.E. Collision Efficiencies for Small Particles with a Spherical Collector at Intermediate Reynolds Numbers. J. Separ. Proc. Technol. **1981**, *2* (1), 29-33.

51. Weber, M.E.; Paddock, D. Interceptional and Gravitational Collision Efficiencies for Single Collectors at Intermediate Reynolds Numbers. J. Colloid Interface Sci. **1983**, *94* (2), 328-335.

52. Reay, D.; Ratcliff, G.A. Removal of Fine Particles from Water by Dispersed Air Flotation: Effects of Bubble Size and Particle Size on Collection Efficiency. Canad. J. Chem. Eng. **1973**, *51*, 178-185.

53. Dobby, G.S.; Finch, J.A. Particle Size Dependence in Flotation Derived from a Fundamental Model of the Capture Process. Int. J. Miner. Process. **1987**, *21*, 241-260.

54. Heindel, T.J.; Bloom, F. Exact and Approximate Expressions for Bubble-Particle Collision. J. Colloid Interface Sci. **1999**, *213*, 101-111.

55. Sutherland, K.L. Kinetics of the Flotation Process. J. Phys. Chem. **1948**, *52*, 394-425.

56. Berg, S.R.; Paulsen, F.G.; Hassler, J.C.; Thompson, E.V. Force-Distance Measurements of Bubble/Particle Interactions. In *4th Research Forum on Recycling*, Château Frontenac, Québec, October 7-9, 1997; CPPA Press: Toronto, 1997; 111-124.

57. Dai, Z.; Fornasiero, D.; Ralston, J. Particle-Bubble Attachment in Mineral Flotation. J. Colloid Interface Sci. **1999**, *217*, 70-76.

58. Derjaguin, B.V.; Dukhin, S.S.; Rulev, N.N. Thin-Film Capillary Hydrodynamic Method in the Theory of Flotation. Colloid J. USSR **1978**, *39* (6), 926-933.

59. Dimitrov, D.S.; Ivanov, I.B. Hydrodynamics of Thin Liquid Films. On the Rate of Thinning of Microscopic Films with Deformable Interfaces. J. Colloid Interface Sci. **1978**, *64* (1), 97-106.

60. Lucassen-Reynders, E.H.; Lucassen, J. Thin Films, Contact Angles, Wetting. In *The Scientific Basis of Flotation*, Ives, K.J., Ed.; Martinus Nijhoff Publishers: The Hague, 1984; 79-109.

61. Nguyen, A.V.; Schulze, H.J.; Ralston, J. Elementary Steps in Particle-Bubble Attachment. Int. J. Miner. Process. **1997**, *51*, 183-195.

62. Rulev, N.N.; Dukhin, S.S. Dynamics of the Thinning of the Film of Liquid Formed Upon the Inertial Impact of a Spherical Particle on the Surface of a Bubble in an Elementary Flotation Act. Kolloid. Z. **1986**, *48* (2), 302-310.

63. Williams, M.B.; Davis, S.H. Nonlinear Theory of Film Rupture. J. Colloid Interface Sci. **1982**, *90* (1), 220-228.

64. Schulze, H.J. Probability of Particle Attachment on Gas Bubbles by Sliding. Adv. Colloid Interface Sci. **1992**, *40*, 283-305.

65. Bloom, F.; Heindel, T.J. An Approximate Analytical Expression for the Probability of Attachment by Sliding. J. Colloid Interface Sci. **1999**, *218*, 564-577.

66. Saffman, P.G. The Lift on a Small Sphere in a Slow Shear Flow. J. Fluid Mech. **1965**, *22*, 385-400.

67. Luttrell, G.H.; Yoon, R.-H. A Hydrodynamic Model for Bubble-Particle Attachment. J. Colloid Interface Sci. **1992**, *154* (1), 129-137.

68. Dobby, G.S.; Finch, J.A. A Model of Particle Sliding Time for Flotation Size Bubbles. J. Colloid Interface Sci. **1986**, *109* (2), 493-498.

69. Jameson, G.J. Experimental Techniques in Flotation. In *The Scientific Basis of Flotation*, Ives, K.J., Ed.; Martinus Nijhoff Publishers: The Hague, 1984; 193-228.

70. Nguyen-Van, A.; Kmet, S.; Schulze, H.J. Collection Events in Flotation: The Quantitative Analysis of the Particle-Bubble Collision and the Attachment of Particle onto Bubble Surface. In *XIX International Mineral Processing Congress*, San Francisco, CA, October 22-27, 1995.

71. Schulze, H.J.; Radoev, B.; Geidel, T.; Stechemesser, H.; Töpfer, E. Investigation of the Collision Process Between Particles and Gas Bubbles in Flotation - A Theoretical Analysis. Int. J. Miner. Process. **1989**, *27* (3/4), 263-278.

72. Schulze, H.J. New Theoretical and Experimental Investigations on Stability of Bubble/Particle Aggregates in Flotation: A Theory on the Upper Particle Size of Floatability. Int. J. Miner. Process. **1977**, *4*, 241-259.

73. Schulze, H.J.; Wahl, B.; Gottschalk, G. Determination of Adhesive Strength of Particles within the Liquid/Gas Interface in Flotation by Means of a Centrifuge Method. J. Colloid Interface Sci. **1989**, *128* (1), 57-65.

74. Hou, M.J.; Hui, S.H. Interfacial Phenomena in Deinking I. Stability of Ink Particle - Air Bubble Aggregates in Flotation Deinking. In *1993 Pulping Conference*, TAPPI Press: Atlanta, GA, 1993; 1125-1142.

75. Plate, H., Ph.D. Thesis, ADW, UVR Freiberg/Sa. Chemnitzer Str. 40, unpublished.

76. Bloom, F.; Heindel, T.J. On the Structure of Collision and Detachment Frequencies in Flotation Models. J. Colloid Interface Sci. In Review.

77. von Smoluchowski, M. Mathematical Theory of the Kinetics of the Coagulation of Colloidal Solutions. Z. physik. Chem. **1917**, *92*, 219-237.

78. Camp, T.R.; Stein, P.C. Velocity Gradients and Internal Work in Fluid Motion. J. Boston Soc. Civil Eng. **1943**, *30*, 219-237.

79. Saffman, P.G.; Turner, T.S. On the Collision of Drops in Turbulent Clouds. J. Fluid Mech. **1956**, *1*, 16-30.

80. Abrahamson, J. Collision Rates of Small Particles in a Vigorously Turbulent Fluid. Chem. Eng. Sci. **1975**, *30*, 1371-1379.

81. Liepe, F.; Möckel, O.H. Untersuchengen zum Stoffvereinigen in flüssiger Phase. Chem. Technol. **1976**, *30*, 205-209.

82. Mika, T.S.; Fuerstenau, D.W. A Microscopic Model of the Flotation Process. In *Proceedings of the 8th International Mineral Processing Congress*, Leningrad, 1968; 246-269.

List of Figures

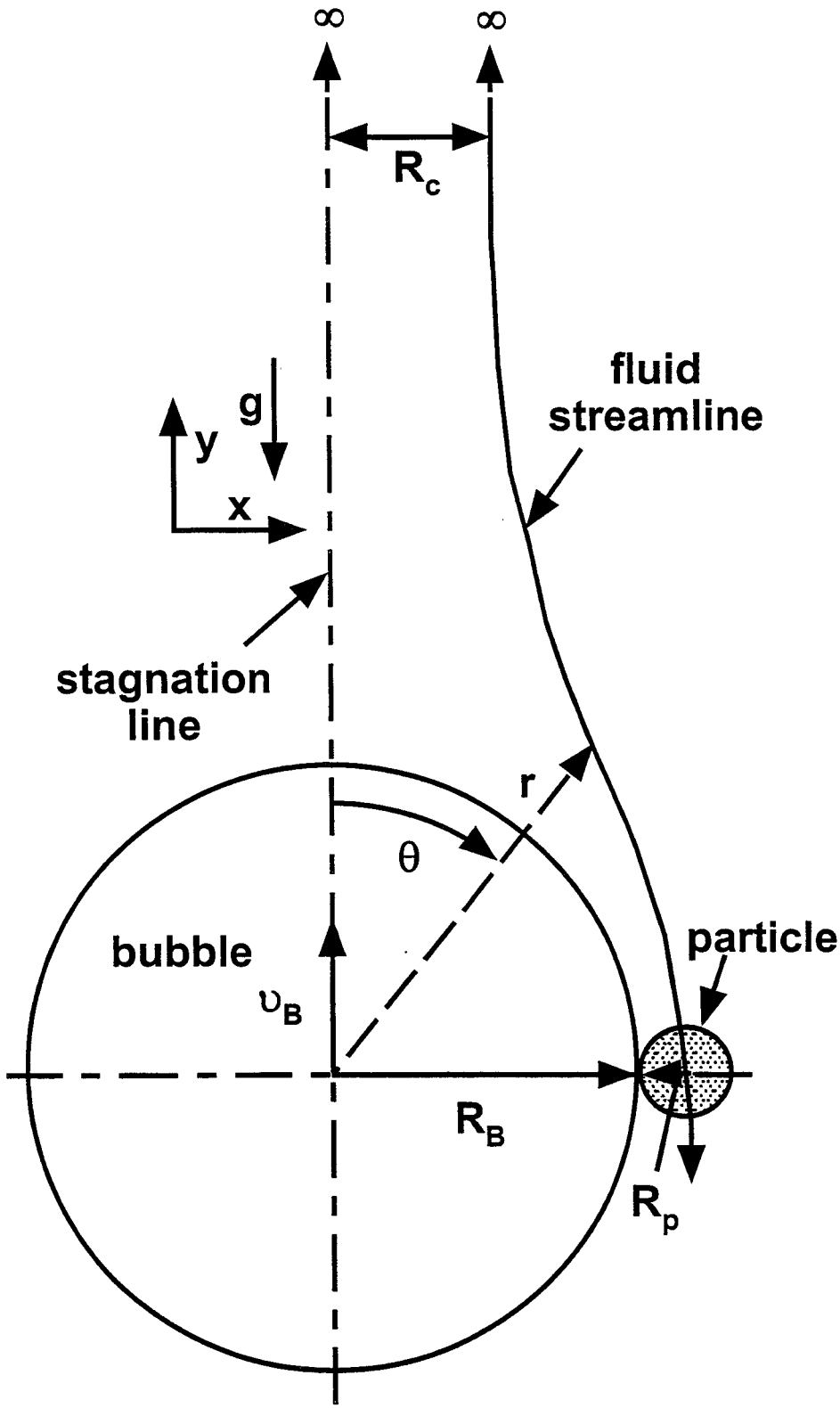
∞
∞
$R_c$
fluid
streamline
g
y
x
stagnation
line
r
θ
bubble
$\upsilon_B$
particle
$R_B$
$R_p$

**Figure 1**

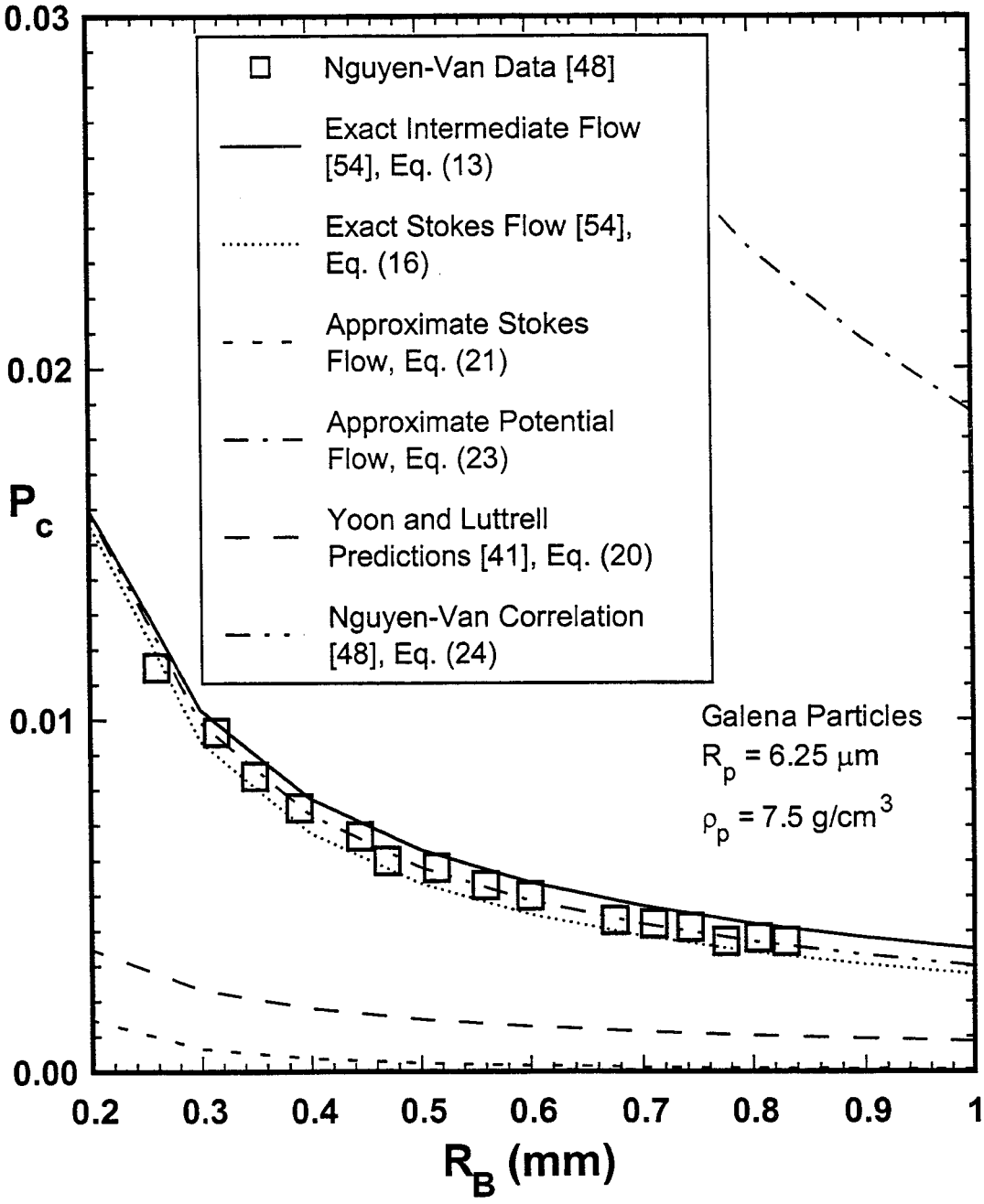
0.03
0.02
0.01
0.00
$P_c$
0.2
0.3
0.4
0.5
0.6
0.7
0.8
0.9
1
$R_B$ (mm)
Nguyen-Van Data [48]
Exact Intermediate Flow [54], Eq. (13)
Exact Stokes Flow [54], Eq. (16)
Approximate Stokes Flow, Eq. (21)
Approximate Potential Flow, Eq. (23)
Yoon and Luttrell Predictions [41], Eq. (20)
Nguyen-Van Correlation [48], Eq. (24)
Galena Particles
$R_p$ = 6.25 μm
$\rho_p$ = 7.5 g/cm$^3$

**Figure 2**

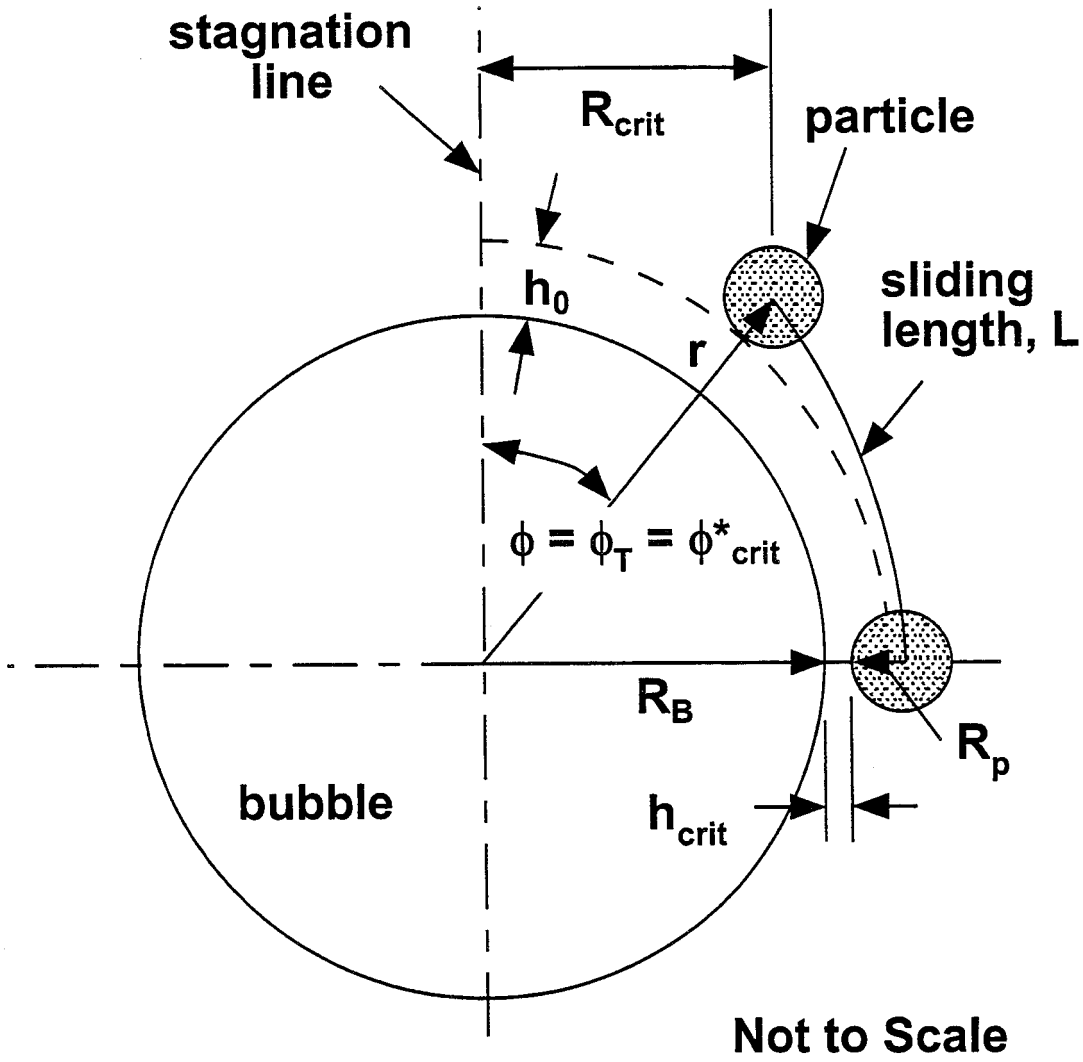
stagnation line
$R_{crit}$
particle
$h_0$
r
sliding length, L
$\phi = \phi_T = \phi^*_{crit}$
$R_B$
$R_p$
bubble
$h_{crit}$
Not to Scale

**Figure 3**

(a) Apparent Particle Weight, $F_{wt} = F_g - F_b$

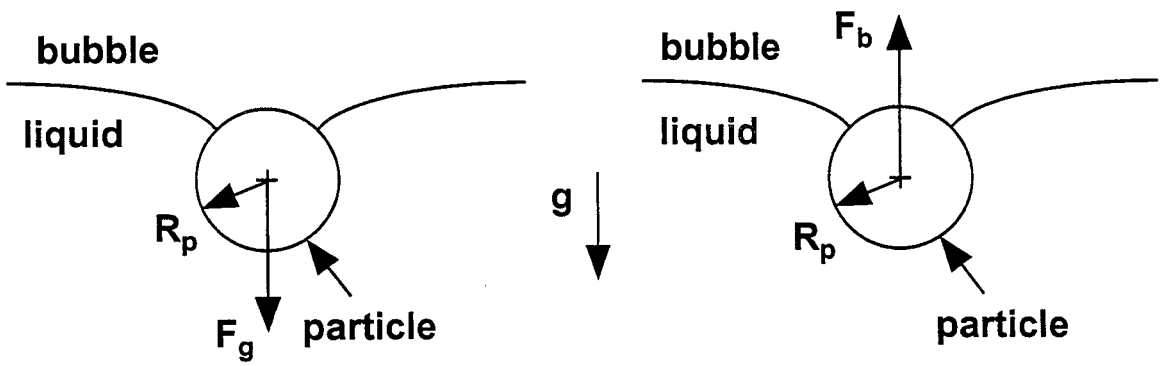


(b) Fluid Drag Force, $F_d$

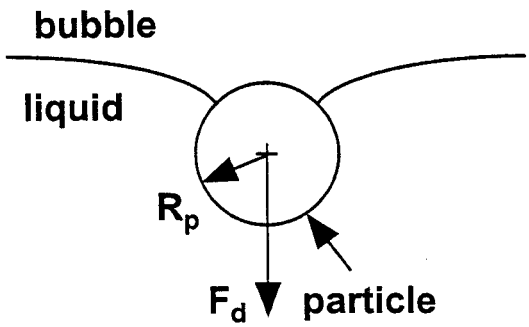


(c) Capillary Pressure Force, $F_\sigma$

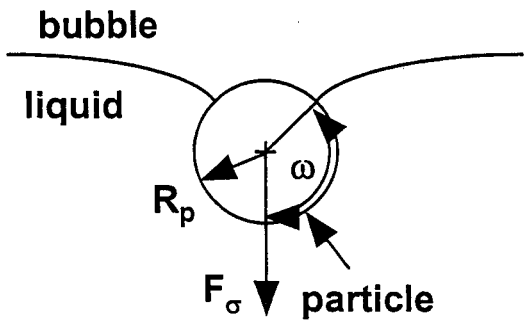


(d) Capillary Force, $F_{ca}$

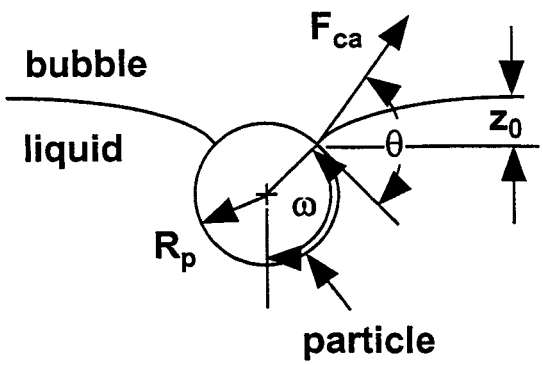


(e) Hydrostatic Pressure Force, $F_{hyd}$

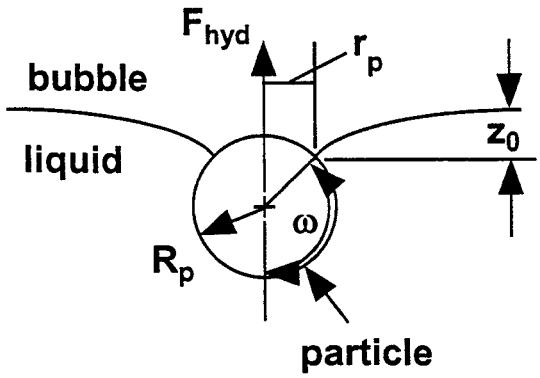


**Figure 4**